Polarization contrast in fluorescence scanning near-field optical reflection microscopy

A. Jalocha and N. F. van Hulst

Applied Optics Group, Department of Applied Physics and MESA Research Institute, University of Twente, P.O. Box 217, 7500 AE Enschede, The Netherlands

Received December 5, 1994; revised manuscript received May 8, 1995

Polarization contrast is presented in fluorescence images of a Langmuir–Blodgett monolayer obtained with a scanning near-field optical microscope operated in reflection. A tapered optical fiber is used both to excite and to collect the fluorescence. The lateral resolution in the reflection fluorescence image is estimated at 200 nm. Shear-force detection controls the tip-to-surface distance and simultaneously gives a topographic map. Direct correlation between topography and the fluorescent domain is thus obtained. We show that the fluorescence is polarized along the molecular orientation in the Langmuir–Blodgett monolayer. Thus we demonstrate the study of the polarization direction in the reflection mode.

1. INTRODUCTION

The basic idea of near-field optical microscopy was suggested near the beginning of the century[1] and demonstrated in 1972[2] with radio-wave frequency, yet scanning near-field optical microscopy (SNOM) was developed only recently.[3,4] The principle of SNOM is the following: a small probe scans the surface of a sample and detects the diffracted light. Thus the lateral resolution depends not on the wavelength but rather on the size of the probe and the distance between the probe and the surface.[1,5–8]

Since the beginning of this new optical microscopy several schemes have been developed with different probes and illumination methods.[9] We can distinguish the reflection and the transmission modes that are suited for opaque, thick, metallic, and for transparent, biological, dielectric samples. Their mutual goal is the extraction of optical properties of the sample with a resolution better than the classical diffraction limit. With the help of a tip to sample separation regulation based on shear-force detection it is possible for the probe to follow the sample contours and simultaneously produce a topographic image.[10,11]

The fluorescence phenomenon is of a great interest in biology and chemistry. In 1986 a SNOM transmission with a lateral resolution of ~50 nm was demonstrated.[12] Since then considerable progress has been achieved. Single molecular detection and characterization have been reached.[13–15] Biological samples such as labeled chromosomes[16] and lipid films[17,18] have been investigated. Although the results open new fields in optical microscopy, this setup is suited for transparent samples only. A reflection configuration was proposed[19–23] in which a tapered optical fiber is used as both an emitter and a collector. In 1992 results obtained with a reflection setup using a SiN probe in combination with a scanning force microscope were presented.[24,25] We present fluorescence images obtained with an equivalent system for control of the tip-to-sample distance.[26] The main advantage of this system compared with conventional far field microscopes or other geometries in a reflection setup[27,28] is the reduction of the photobleaching. We investigated the fluorescence polarization characteristics of Langmuir–Blodgett films as also reported in classical microscopy[29,30] and in SNOM transmission.[17,18] Our results are promising: We demonstrate that optical contrast methods of conventional microscopy can be applied in the SNOM reflection setup that will be helpful in solid-state physics and studies of nontransparent surfaces.

2. SAMPLE

Ultrathin lipid films have several industrial applications[28] but also are ideal test structures for near-field microscopy. We investigated a diethylene glycol diamine pentacosadiynoic amide DPDA monolayer polymerized by UV radiation. Its preparation by Langmuir–Blodgett techniques is the same as described previously.[17] The transfer speed is 50 μm/s vertically, with a transfer ratio close to 1. Thus a polymerized DPDA monolayer with a thickness of 6 nm is obtained on the surface of a glass slide. The layer is composed of domains, and its crystallinity gives rise to a high anisotropy, in which each domain has a high optical density and an intense anisotropic fluorescence.[28] The domain geometry is not regular, and the domain size can reach several square micrometers. In each domain the absorption and emission moments are oriented uniformly. The absorption band is in the green and the emission in the red.[17,18]

3. DESCRIPTION OF THE INSTRUMENT

The experimental setup is shown in Fig. 1. An Ar^+ laser ($\lambda = 514$ nm) is focused into a multimode fiber. A polarizer controls the incoming beam polarization. A dichroic mirror ($\lambda = 560$ nm) and a high-pass filter ($\lambda > 590$ nm) are used to separate the excitation beam and the fluorescence beam coming from the sample. An additional analyzer controls the output polarization. To use the fiber as a probe, we reduce the fiber diameter by pulling with a commercial instrument (Sutter P2000). The extremity size can reach less than 100 nm. The fiber is used both

0740-3224/95/091577-04$06.00

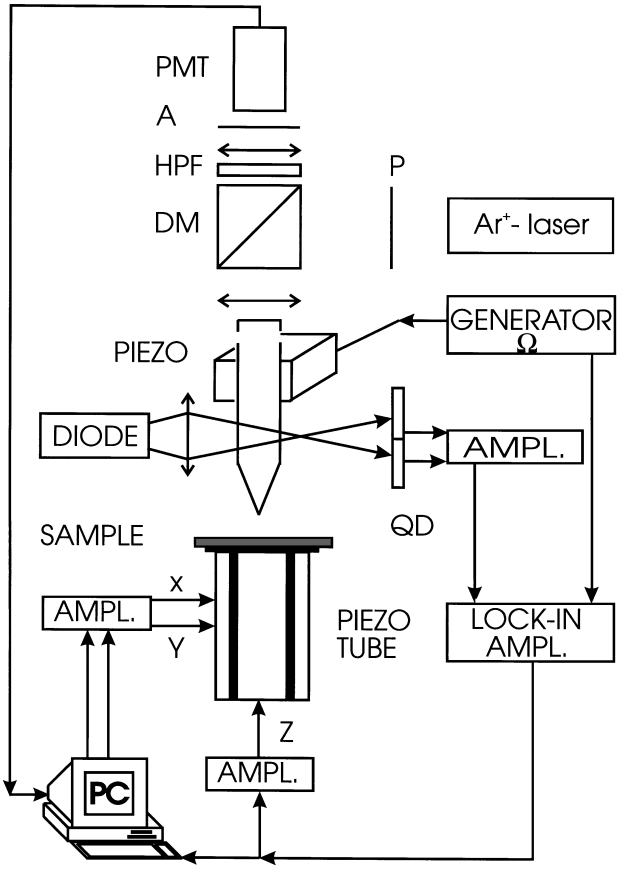

Fig. 1. Reflection setup for fluorescence and shear force detection. The high-pass filter (HPF) blocks $\lambda_{exc} = 514$ nm. Only the fluorescence signal $\lambda_{fluo} > 590$ nm is recorded. QD, quadrant detector; PMT, photomultiplier tube; PC, personal computer; DM, dichroic mirror; A, analyzer; P, polarizer; PIEZO, piezoceramic.

as an emitter for the exciting wavelength and as a collector for the fluorescence.[24] The detected intensity not only is a function of the probe brightness but depends on the coupling between the probe and the backward fluorescence. We chose to use a nonmetallized tip for this configuration to minimize the losses. However, better resolution was obtained with an aluminum-coated tip for transmission. Our choice is a compromise between detected level and expected resolution.

We implemented external shear-force detection to control the tip-to-sample distance.[10,11] One end of the fiber is attached to a piezoceramic, which vibrates at the first resonance frequency of the mechanical system (typically 5 kHz). The dither amplitude is 30 nm. A laser diode is focused near the extremity. A quadrant detector measures the vibration amplitude.[17] When the tip approaches the surface, the vibration is damped to zero amplitude within 10 nm before the contact point. This behavior can be explained by the force gradient that acts in the vicinity of the surface. Thus the amplitude of the dither vibration changes. The amplitude is monitored and the shear-force signal is kept constant by feedback on the piezotube supporting the sample system. The probe follows the contours of the surface, and a topographic map is produced.

A piezotube permits sample displacement in the x and y directions with a maximum scale of 20 μm^2. A personal computer is used to generate the scan pattern and to acquire the fluorescence and shear-force signals. The data-acquisition frequency is 300 Hz.

4. RESULTS AND DISCUSSION

Figure 2(a) shows the shear-force and Fig. 2(b) the fluorescence images of the DPDA film. The scan area

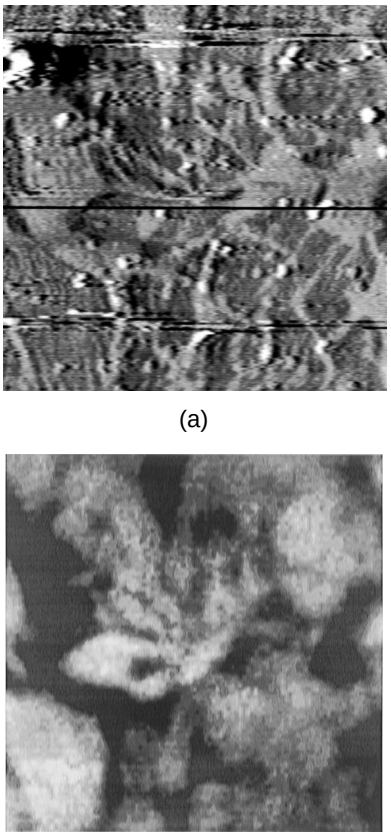

(a)

(b)

Fig. 2. 10.4 μm $\times$ 10.4 μm (52-nm pixel size) images of DPDA. (a) On the shear-force image the contrast is inverted with respect to the topography, as explained in the text. (b) Corresponding near-field fluorescence image where different film domains appear bright.

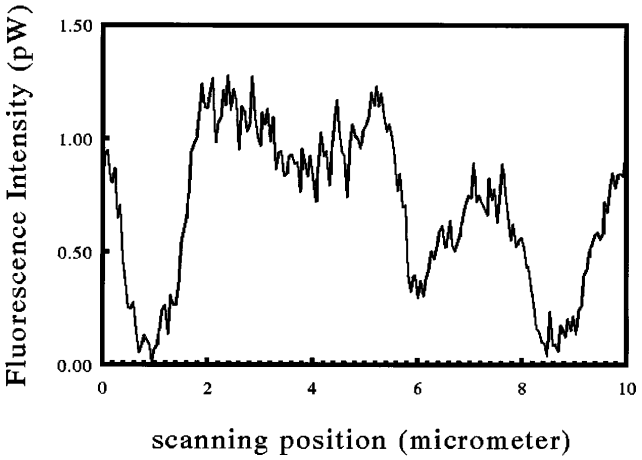

Fig. 3. Fluorescence line intensity of the optical image of Fig. 2(b). The pixel size is 52 nm. We can distinguish the fluorescence domains.

Fig. 4. (a) Shear-force and (b), (c) fluorescence images of the DPDA film. The image size is 10.4 μm × 10.4 μm, and the pixel size is 52 nm. The two fluorescence images are obtained with different input polarizations, perpendicular to each other. The relative intensity of several domains changes with the input polarization. This behavior is due to the high anisotropy of the DPDA film.

is 10.4 μm × 10.4 μm, with a pixel size of 51 nm. Figure 2(b) displays the total fluorescence without an analyzer. By comparing both images one can see that the shear-force contrast is inverted with respect to the topography. The darker areas in Fig. 2(a) show as a strong fluorescence signal in Fig. 2(b), which means that those areas are film domains. In this case not only does the shear-force image contribute to the topographic map but, depending on the nature of the surface, chemically specific forces play a role too. An aluminum layer of thickness comparable with that of the film (12 nm) has been used with the same system, and no inverted contrast in the shear-force image was seen. Thus this effect cannot be explained as an artifact of the feedback system resulting from the small height of the film. The shear-force image in the feedback displays the piezo voltage needed to keep the effective shear-force signal constant. Apparently the shear-force damping mechanism is weaker on polymer than on glass. As a result the tip has to be closer to the polymer surface than to the glass surface to maintain an equivalent shear-force signal despite the 6-nm topographic height of the polymer. It gives rise to an inverted contrast when the tip is scanning Langmuir–Blodgett films. Dust appears on the film with positive contrast. This behavior agrees with our explanation. The same film studied by SNOM for transmission with a metallized tip[17,18] did not display this inverted contrast. Apparently forces measured by the shear-force technique are dependent on both sample and tip composition.

The multimode fiber does not preserve the linear polarization, and it gives rise to excitation of all domains. Yet two domains appear to be more fluorescent. We measured the fluorescence signal at 1.3 pW. The degree of polarization for the exciting beam after transmission through the tip, $P = (I_{max} - I_{min})/(I_{max} + I_{min})$, was measured at $P = 0.5$ with $I_{max} = 1$ μW, enough to show the different domain emissions. For successive images the analyzer is kept in a position where the contrast is maximum.

To estimate the resolution of the fluorescence image, we have plotted an intensity profile in Fig. 3. We define the resolution as the width between maximum − 20% and minimum + 20%. An average resolution value of ~200 nm is estimated.[26] Figure 4 shows scans of another part of the same sample. The scan area is 10.4 μm × 10.4 μm for 200 × 200 pixels. The shear-force image [Fig. 4(a)] shows that it is composed of different topographic domains. The fluorescence images in Figs. 4(b) and 4(c) were obtained for two different input polarizations whose directions were perpendicular. The fluorescence signal depends on the input polarization and on both absorption and emission moments. This is inherent in the high-fluorescence anisotropy of the domains. The absorption and emission moments are oriented parallel to the polymer backbone, and each distinct domain has a uniform distribution that is parallel to the plane. The fluorescence level is maximum when the polarization input is parallel to the absorption moment of the domain that depends on its specific property. Domains with perpendicular orientation appear with inverted levels between Figs. 4(b) and 4(c).

In Fig. 5 we have plotted the shear force [Fig. 5(a)] and fluorescence [Figs. 5(b) and 5(c)] lines for the position shown by the line in Fig. 4(a). The fluorescence signal clearly depends on the incident polarization. However, the illumination polarization is not totally linear. Thus the part of the light that is not linearly polarized exits all domains and gives a background level.

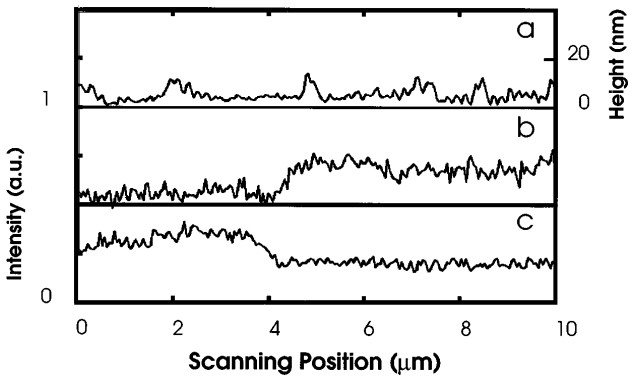

Fig. 5. (a) Shear-force profile and (b), (c) fluorescence intensities with mutually perpendicular polarization corresponding to Figs. 4(a), 4(b), and 4(c), respectively. The line in (a) corresponds to the position of the line in Fig. 4(a). The polarization contrast is clearly demonstrated.

5. CONCLUSION

We have presented what are to our knowledge the first fluorescence measurements with polarization contrast obtained with a reflection-scanning near-field microscope. A tapered nonmetallic optical fiber is used both as an emitter for the exciting wavelength and as a detector of the reflected signal. We demonstrated that we can distinguish fluorescent and nonfluorescent areas with a resolution of ~200 nm. Using the anisotropic properties of Langmuir–Blodgett films, we demonstrated polarization contrast. It is thus possible to characterize domains with perpendicular absorption moments. We showed a specific behavior of the shear-force regulation that is used to control the tip-to-sample separation. This signal seems to be dependent on the topography and also on the chemical nature of the surface. However, it should be studied in more detail to give a rigorous explanation. These optical results are promising because they are superior to those from other systems. This reflection mode is versatile and can be used on either an opaque, thick sample or on a dielectric, transparent sample. The wavelength excitation coming from the tip illuminates a small part of the sample and, compared with that from reflection setup that uses external illumination, it reduces the photobleaching process in fluorescence measurements. In the future we intend to study the use of a metallic tip, which could improve the lateral resolution.

ACKNOWLEDGMENTS

We thank Marco Moers for his valuable comments and helpful discussions. The Langmuir–Blodgett films samples were prepared by Uli Hoffmann and Hermann E. Gaub of the Technical University of Münich. This research was supported by the European Commission for Research (contract ERBCHGCT 920049).

REFERENCES

1. E. A. Synge, "Method for extending microscopic radiation into the ultra-microscopic region," Philos. Mag. **6,** 356–358 (1928).
2. E. A. Ash and G. Nicholls, "Super-resolution aperture scanning microscope," Nature (London) **237,** 510–512 (1972).
3. U. Ch. Fischer, U. Dürig, and D. W. Pohl, "Near-field optical scanning microscopy and enhanced spectroscopy with submicron apertures," Scan. Microsc. Suppl. **1,** 47–52 (1987).
4. D. W. Pohl, U. Ch. Fischer, and U. Dürig, "Scanning near-field optical microscopy," J. Microsc. **152,** 853–861 (1988).
5. G. A. Massey, "Microscopy and pattern generation with scanned evanescent waves," Appl. Opt. **23,** 658–660 (1984).
6. C. Girard and M. Spajer, "Model for reflection near-field optical microscopy," Appl. Opt. **29,** 3726–3733 (1990).
7. A. Dereux, J-P. Vigneron, P. Lambin, and A. A. Lucas, "Theory of near-field optics with application to SNOM and optical binding," Physica B **175,** 65–67 (1991).
8. D. van Labeke and D. Barchiesi, "Scanning-tunnelling optical microscopy: a theoretical macroscopic approach," J. Opt. Soc. Am. A **9,** 732–739 (1992).
9. D. W. Pohl, in *Advances in Optical and Electron Microscopy*, C. J. R. Sheppard and T. Mulvey, ed. (Academic, San Diego, Calif., 1991), pp. 243–312.
10. E. Betzig, P. L. Finn, and J. S. Weiner, "Combined shear force and near-field scanning optical microscopy," Appl. Phys. Lett. **60,** 2484–2486 (1992).
11. R. Toledo-Crow, P. C. Yang, Y. Chen, and M. Vaez-Iravani, "Near-field differential scanning optical microscope with atomic force regulation," Appl. Phys. Lett. **60,** 2957–2959 (1992).
12. E. Betzig, A. Lewis, A. Harootunian, M. Isaacson, and E. Kratschmer, "Near-field scanning optical microscopy," Biophys. J. **49,** 269–279 (1986).
13. E. Betzig and R. Chichester, "Single molecules observed by near-field scanning optical microscopy," Science **262,** 1422–1424 (1993).
14. R. Kopelman and W. Tan, "Near-field optics: imaging single molecules," Science **262,** 1382–1384 (1993).
15. W. P. Ambrose, P. M. Goodwin, J. C. Martin, and R. A. Keller, "Alterations of single molecule fluorescence lifetimes in near-field optical microscopy," Science **265,** 364–367 (1994).
16. N. F. van Hulst, M. H. P. Moers, and E. Borgonjon, "Applications of near field optical microscopy," in *Proceedings of the Workshop on Photon and Local Probes*, in NATO ASI series E (Kluwer, Dordrecht, The Netherlands, to be published).
17. M. H. P. Moers, N. F. van Hulst, A. G. T. Ruiter, and B. Bölger, "Optical contrast in near-field techniques," Ultramicroscopy **57,** 298–302 (1995).
18. M. H. P. Moers, H. E. Gaub, and N. F. van Hulst, "Polydiacetylene monolayers studied with a fluorescence scanning near-field optical microscope," Langmuir **10,** 2774–2777 (1994).
19. D. Courjon, J. M. Vigoureux, M. Spajer, K. Sarayeddine, and S. Leblanc, "External and internal reflection near-field microscopy: experiments and results," Appl. Opt. **29,** 3734–3740 (1990).
20. M. Spajer, D. Courjon, K. Sarayeddine, A. Jalocha, and J. M. Vigoureux, "Microscopie en champ proche par reflexion," J. Phys. III **1,** 1–12 (1991).
21. M. Spajer and A. Jalocha, "The reflection near field optical microscope an alternative to STOM," in *Near Field Optics*, D. W. Pohl and C. Courjon, eds. (Kluwer, Dordrecht, The Netherlands, 1993), pp. 87–94.
22. A. Jalocha and C. Pieralli, "A scanning optical profilometer using the SNOM architecture," Pure Appl. Opt. **3,** 793–804 (1994).
23. S. Berntsen, E. Bolezhovnaya, and S. Bolezhovnyi, "Macroscopic self-consistent model for external-reflection near-field microscopy," J. Opt. Soc. Am. A **10,** 878–885 (1993).
24. N. F. van Hulst, M. P. H. Moers, O. F. J. Noordman, T. Faulkner, F. B. Segerink, K. O. van der Werf, B. G. de Grooth, and B. Bölger, "Operation of a scanning near-field optical microscope in reflection in combination with a scanning force microscope," in *Scanning Probe Microscopies*, S. Manne, ed., Proc. Soc. Photo-Opt. Instrum. Eng. **1639,** 36–43 (1992).
25. N. F. van Hulst, M. H. P. Moers, and B. Bölger, "Near-field optical microscopy in transmission & reflection modes in combination with force microscopy," J. Microsc. **171,** 95–105 (1993).
26. A. Jalocha and N. F. van Hulst, "Dielectric and fluorescent samples imaged by scanning near-field optical microscopy in reflection," Opt. Commun. (to be published).
27. P. J. Moyer and M. A. Paesler, "Shear force/reflection near-field scanning optical microscopy," in *Scanning Probe Microscopies II*, C. C. Williams, ed., Proc. Soc. Photo-Opt. Instrum. Eng. **1855,** 58–66 (1993).
28. H. Bielefeld, I. Hörsch, G. Krausch, M. Lux-Steiner, J. Mlynek, and O. Marti, "Reflection-scanning near-field optical microscopy and spectroscopy of opaque samples," Appl. Phys. A **59,** 103–108 (1994).
29. B. M. Goettgens, R. W. Tillmann, M. Radmacher, and H. E. Gaub, "Molecular order in polymerizable Langmuir–Blodgett films by microfluorescence and scanning force microscopy," Langmuir **8,** 1768–1774 (1992).
30. R. W. Tillmann, M. Radmacher, H. E. Gaub, P. Kenney, and H. O. Ribi, "Monomeric and polymeric molecular films from the diethylene glycol diamine pentacosadiynoic amide," J. Phys. Chem. **97,** 2928–2932 (1993).